104 (2025) 104965

Contents lists available at ScienceDirect

Poultry Science

journal homepage: www.elsevier.com/locate/psj

Co-exposure to ammonia and lipopolysaccharide-induced impaired energy metabolism via the miR-1599/HK2 axis and triggered autophagy, ER stress, and apoptosis in chicken cardiomyocytes

Zhiyu Hao [a], Minna Qiu [a], Yuhao Liu [a], Yuhang Liu [a], Minghang Chang [a], Xiumei Liu [d], Yan Wang [e], Wei Sun [a,**], Xiaohua Teng [a,*], You Tang [b,c,**]

[a] College of Animal Science and Technology, Northeast Agricultural University, Harbin 150000, China
[b] College of Electrical and Information Engineering, JiLin Agricultural Science and Technology University, Jilin 132101, China
[c] College of Information Technology, Jilin Agricultural University, Changchun, Jilin, 132101, China
[d] College of Life Sciences, Yantai University, Yantai, 264005, China
[e] School of Public Health, Beihua University, Jilin, 132013, China

ARTICLE INFO

Keywords:
Ammonia and lipopolysaccharide
Energy metabolism
Autophagy
Endoplasmic reticulum stress
Apoptosis

ABSTRACT

Ammonia (NH_3) and lipopolysaccharide (LPS), common pollutants in poultry farming environments, pose significant health risks by disrupting cellular processes. Although previous studies have demonstrated the individual effect of NH_3 or LPS on human and animal health, the mechanisms underlying their combined impact on chicken heart tissue remain poorly understood. In this study, we established a chicken cardiotoxicity model to investigate the effects of NH_3 and/or LPS exposure on energy metabolism, autophagy, endoplasmic reticulum (ER) stress, and apoptosis in cardiomyocytes. Our findings indicated that exposure to NH_3 or/and LPS reduced ATPase activity and ATP content, led to the downregulation of HK2, PK, PDHX, and SDH, and upregulation of AMPK, resulting in impaired energy metabolism in chicken cardiomyocytes. Additionally, we found the gga-miR-1599/HK2 axis as a key regulator involved in NH_3 or/and LPS-induced energy metabolism impairment. The impairment in energy metabolism activated the AMPK/mTOR pathway, which subsequently triggered autophagy, evidenced by the upregulation of Beclin, LC3-I, and LC3-II. Furthermore, decreased mTOR expression induced ER stress, as indicated by the upregulation of key markers such as ATF6, GRP78, IRE1, and PERK. ER stress, in turn, increased CHOP expression, which downregulated Bcl-2 and upregulated Bim, resulting in elevated levels of Bax, caspase-9, and caspase-3, ultimately triggering apoptosis. This study provides valuable insights into the mechanisms of NH_3 and LPS co-exposure on poultry heart tissue and identifies potential molecular targets for mitigating these adverse effects.

Introduction

Ammonia (NH_3) and lipopolysaccharide (LPS) are widespread environmental pollutants in modern poultry farming, presenting significant risks to animal health (Smit et al., 2017; Wyer et al., 2022). NH_3, a colorless and irritant gas, is recognized as a primary atmospheric pollutant. Research indicated that NH_3 pollution primarily originates from agricultural activities, especially poultry production (Van Damme et al., 2018). Due to its critical role in PM2.5 aerosol formation, NH_3 exposure poses considerable health hazards to humans and animals (Wyer et al., 2022). High concentrations of NH_3 impaired the immune system in chickens, affecting tissues including the heart (Xing et al.,

Abbreviations: NH_3, Ammonia; LPS, lipopolysaccharide; ER, endoplasmic reticulum; TCA cycle, tricarboxylic acid cycle; HK2, hexokinase 2; PK, pyruvate kinase; PDHX, pyruvate dehydrogenase complex component X; SDH, succinate dehydrogenase; AMPK, adenosine 5'-monophosphate (AMP)-activated protein kinase; LC3, microtubule associated protein 1 light chain 3; mTOR, mechanistic target of rapamycin kinase; PERK, the protein kinase RNA-like ER kinase; ATF6, activating transcription factor 6; IRE1, inositol-requiring enzyme 1; GRP78, glucose-regulated protein 78; CHOP, C/EBP homologous protein; miRNA, MicroRNA; PPI, protein-protein interaction.

* Corresponding author at: College of Animal Science and Technology, Northeast Agricultural University, Harbin 150000, China.
** Corresponding authors.
E-mail addresses: sun@neau.edu.cn (W. Sun), xiaohuateng@neau.edu.cn (X. Teng), tangyou@jlnku.edu.cn (Y. Tang).

https://doi.org/10.1016/j.psj.2025.104965
Received 14 November 2024; Accepted 28 February 2025
Available online 1 March 2025
0032-5791/© 2025 The Authors. Published by Elsevier Inc. on behalf of Poultry Science Association Inc. This is an open access article under the CC BY-NC-ND license (http://creativecommons.org/licenses/by-nc-nd/4.0/).

2019), spleen (Han et al., 2020), and thymus (Chen et al., 2020). LPS, an endotoxin and a component of Gram-negative bacterial cell walls, is prevalent in air, water, feed, and waste, inducing various cytotoxic effects, including endoplasmic reticulum (ER) stress and apoptosis (Ghareeb et al., 2016). Despite the prevalence of NH_3 and LPS in poultry environments, systematic studies on their combined effects in poultry remain limited.

Cardiomyocytes have high and variable energy demands, which increase with contractile stress. To meet these demands, ATP production in cardiomyocytes predominantly relies on mitochondrial glucose oxidation. Glucose is metabolized through glycolysis and the tricarboxylic acid cycle (TCA cycle), leading to ATP production for cardiac function (Kolwicz et al., 2013). Environmental pollutants are known to disrupt energy metabolism in animals. For example, Chi et al. (2018) reported that hydrogen sulfide exposure affected the mRNA expression of hexokinase 2 (HK2), pyruvate kinase (PK), pyruvate dehydrogenase complex component X (PDHX), and succinate dehydrogenase (SDH), disrupting energy metabolism in chicken peripheral lymphocytes. Zhang et al. (2022c) demonstrated that NH_3 exposure affected HK2 and adenosine 5'-monophosphate (AMP)-activated protein kinase (AMPK) mRNA expression, leading to energy metabolism disorders in pig hearts. Chen et al. (2023a) found NH_3-induced mitochondrial damage in chicken splenic lymphocytes, with affected expression levels of HK2, PK, and SDH mRNA, leading to metabolic imbalance.

Autophagy is closely associated with energy metabolism, particularly as a critical cellular response to energy deprivation (Yang et al., 2019). Environmental pollutants can induce autophagy by disrupting energy metabolism. For example, cadmium exposure has been shown to affect the mRNA expression of HK2, PK, PDHX, SDH, microtubule-associated protein 1 light chain 3 (LC3), Beclin, and mechanistic target of rapamycin kinase (mTOR), causing energy metabolic disorders and autophagy in chicken ovaries (Wang et al., 2018a). Excessive copper exposure affected AMPK, Beclin, LC3-I, LC3-II, and mTOR expression, inducing renal energy metabolic disorders in broilers and mediating autophagy through the AMPK-mTOR pathway (Liao et al., 2020). Notably, mTOR serves as a key regulator of both energy metabolism and autophagy, suggesting a crucial role in pollutant-induced cellular responses (Gargalionis et al., 2024).

ER plays a crucial role in maintaining cellular homeostasis, acting as the primary site for protein synthesis, folding, and quality control. Disruption of ER function leads to a condition known as ER stress, which, if prolonged or severe, can trigger apoptosis—an orchestrated form of cell death (Zhang et al., 2022b). Current research identifies three key signaling pathways involved in the regulation of ER stress: the protein kinase RNA-like ER kinase (PERK), activating transcription factor 6 (ATF6), and inositol-requiring enzyme 1 (IRE1) pathways. These pathways are activated upon dissociation from glucose-regulated protein 78 (GRP78), initiating an adaptive response aimed at restoring ER function (Zhang et al., 2022b). However, when ER stress persists, the C/EBP homologous protein (CHOP) is upregulated, further promoting apoptosis as a response to sustained stress (Chen et al., 2023c). Environmental pollutants have been shown to induce ER stress and apoptosis across chicken tissues and cells. For example, lead exposure induced apoptosis via ER stress in chicken kidneys (Wang et al., 2018b). Mercuric chloride exposure triggered apoptosis in embryonic chicken renal cells through ER stress pathways (Ma et al., 2020). Copper exposure induced ER stress-driven apoptosis in chicken cardiomyocytes (Ma et al., 2023). Moreover, there is a relationship between energy metabolism disorders and ER stress. Alterations in cellular energy metabolism can impair ER function, thereby exacerbating ER stress and triggering cell death (Ghemrawi et al., 2018). For instance, Chen et al. (2015) demonstrated that cadmium-induced energy imbalance in rat cardiomyocytes led to both ER stress and apoptosis. Likewise, Pan et al. (2023) found that abamectin exposure caused energy metabolic disturbances in carp spleen cells, leading to ER stress and subsequent apoptosis.

MicroRNAs (miRNAs) are evolutionarily conserved, single-stranded, non-coding RNAs that regulate gene transcription or translation and play essential roles in cellular growth, differentiation, and development (Yang et al., 2016). Emerging research highlighted miRNAs as critical regulators of energy metabolism, particularly in response to environmental factors. For example, miR-210 was associated with nickel-induced alterations in energy metabolism in Neuro-2a cells (He et al., 2014), while other miRNAs mediate energy metabolism disturbances in TM4 Sertoli cells under combined arsenic and lead exposure (Zheng et al., 2024). Despite the evidence that NH_3 or LPS has an impact on human and animal health, the mechanisms by which combined NH_3 and LPS exposure affects chicken cardiac tissue remain unexplored. Transcriptomic analyses from our laboratory found gga-miR-1599 as differentially expressed in a chicken cardiac toxicity model induced by NH_3 exposure. Thus, this study aims to determine whether NH_3 or/and LPS affect cardiomyocyte energy metabolism, investigate the role of gga-miR-1599 in NH_3 or/and LPS-induced energy metabolism regulation, and explore whether this regulation of energy metabolism triggers autophagy, ER stress, and apoptosis in chicken cardiomyocytes.

Materials and methods

Experimental animals

In our experiments, all procedures involving broilers were conducted in accordance with the Animal Care and Use Committee of Northeast Agricultural University (Harbin, China). Eighty 1-day-old broilers (Weiwei Co. Ltd., Harbin, China) were randomly assigned to two groups of 40 each: the low NH_3 group (5 mg/m^3 ammonia during weeks 1-6) and the high NH_3 group (20 mg/m^3 NH_3 during weeks 1-3 and 45 mg/m^3 NH_3 during weeks 4-6). NH3 concentration in the high NH_3 group was set based on actual concentration in broiler production (Osorio Hernandez et al., 2016; Vučemilo et al., 2007). These broilers were housed in environmentally controlled chambers at the Experimental Animal Center of the College of Veterinary Medicine, Northeast Agricultural University (Harbin, China). During the 42-day experiment, the broilers were allowed to feed and water freely. After 42 days of feeding, the low ammonia group randomly selected 20 broilers for intraperitoneal injection with LPS (200 mg/kg), designated as group P, while the remaining 20 chickens served as the control group, designated as group C. Similarly, in the high ammonia group, 20 broilers were randomly selected for intraperitoneal injection with LPS, designated as the group NP, while the remaining 20 chickens served as a single ammonia group, designated as the group N. After 12 hours of infection, the broilers were euthanized; some heart tissues were extracted and fixed in 10 % formalin, while the rest of the tissues were immediately frozen in liquid nitrogen for 1 h and then stored in a refrigerator at -80° C.

Histological observation of heart tissues

First, the heart tissues, fixed in 2.5 % glutaraldehyde solution, were removed, washed in 0.1 M sodium phosphate buffer at 4° C for 1 hour, and dyed in 1 % sodium tetrasodium phosphate buffer at 4° C for another hour. The tissues were then dehydrated in 50 %, 70 %, 90 %, and 100 % ethanol for 10 minutes each, followed by washing with pure acetone and soaking in the embedding solution overnight. The samples were embedded in epoxy resin and subsequently sectioned into ultra-thin slices. The ultra-thin sections were stained with uranyl acetate and lead citrate, and the ultrastructure of chicken hearts was examined using a transmission electron microscope (Eclipse 80i/90i, Nikon, Tokyo, Japan).

Measurement of ATPase activity and ATP content

The homogenized tissues were centrifuged at 4 °C, 1000 g for 15 min,

and the supernatants were collected for measurement of ATPase activity and ATP content. Four ATPase indicators, including Na-K-ATPase, Ca^{++2+}-ATPase, Mg^{2+}-ATPase, and $Ca2^{+}$-Mg^{2+}-ATPase, as well as ATP content were carried out by assay kits (Nanjing Jiancheng Bioengineering Institute, China, A016-2 and A095-1-1). The detection was performed according to the instructions given by the reagent company. An absorbance microplate reader (SpectraMax®ABS 00254, Molecular Devices, Shanghai, China) was applied.

Real-time quantitative PCR analysis of genes on miRNA level and mRNA level

According to the manufacturer's instructions (TaKaRa, Japan), total RNA was extracted from heart tissues using Trizol reagent, and the quality and concentration of RNA were measured at a 260/280 wavelength using a microspectrophotometer (Nano-400, Allsheng Instruments Co., Ltd, China). Additionally, the miRNA First Strand cDNA Synthesis Kit (Sangon Biotech (Shanghai) Co., Ltd, China) was used for the reverse transcription of miRNA using the tailing reaction method. Reverse transcription of mRNA was performed using the Fast King cDNA First Strand Synthesis Kit (Tiangen Biotech Co. Ltd., China). To detect mRNA expression, RT-qPCR was conducted with FastStart Universal SYBR Green Master (ROX) (Roche, Switzerland) using the QuantStudio 3 System (Thermo Fisher, America). The reaction mixture (20 μL) contained 10 μL of FastStart Universal SYBR Green Master (ROX), 0.6 μL each of forward and reverse primers (10 μM), 2 μL of template cDNA, and 6.8 μL of RNase-free water. To assess miRNA expression, RT-qPCR was performed with the MicroRNAs qPCR Kit (SYBR Green Method) using the QuantStudio 3 System (Thermo Fisher, America). This reaction mixture (20 μL) included 10 μL of 2×miRNA qPCR master mix, 0.5 μL each of forward and reverse primers (10 μM), 2 μL of template cDNA, and 7 μL of RNase-free water. In our experiment, melting curve analysis indicated that each final product was singular. The transcript levels of miRNA and mRNA were analyzed using the $2^{-\Delta\Delta Ct}$ method (Che et al., 2025; Ma et al., 2023). The primers used in our experiment are presented in Table 1, with U6 serving as the internal reference for miRNA and β-actin as the internal reference for mRNA (Zhou et al., 2025; Liu et al., 2020). PCR specificity was determined using BLAST (https://blast.ncbi.nlm.nih.gov/Blast.cgi).

Protein-protein interaction (PPI) analysis

We used the STRING protein interaction data base (http://string-db.org) to construct the PPI network of energy metabolism, autophagy, ER stress and apoptosis-related genes. Using the online STRING software, PPI confidence scores > 0.7 were defined as significant interactions. The PPI network was visualized using Cystoscape software. Within the PPI network, the term "degree" indicates the number of connections a

Table 1
Specificity primers used in the experiment.

Gene	Primer sequence	Primer length (bp)
U6	Forward 5′-CACGCAAATTCGTGAAGCGTTCCA-3′	24
	Reverse by Sangon Biotech (Shanghai) Co., Ltd.	
miR-1599	Forward 5′-GCGCCGGAGGGAGGAAAAAAAAAAA-3′	25
	Reverse by Sangon Biotech (Shanghai) Co., Ltd.	
β-actin	Forward 5′-CCGCTCTATGAAGGCTACGC-3′CCGCTCTATGAAGGCTACGCCCGCTCTATGAAGGCTACGCCTCTCGGCTGTGGTGGTGAA	20
	Reverse 5′-CTCTCGGCTGTGGTGGTGAA-3′	20
BCL-2	Forward 5′-ATCCCATCCTCCGTTGTCCT-3′	20
	Reverse 5′-ATCGTCGCCTTCTTCGAGTT-3′	20
Bim	Forward 5′-AAGAGTTGCGGCGTATTGGAGAC-3′	23
	Reverse 5′-ACCAGGCGGACAATGTAACGTAAC-3′	24
Bax	Forward 5′-TATGGGACACCAGGAGGGTA-3′	20
	Reverse 5′-CGTAGACCTTGCGGATAAAGC-3′	21
Caspase-3	Forward 5′-TACCGGACTGTCATCTCGTTCAGG-3′	24
	Reverse 5′-ACTGCTTCGCTTGCTGTGATCTTC-3′	24
Caspase-9	Forward 5′-CAAGGTGAGTGGCTCGTGGTAC-3′	22
	Reverse 5′-CCGAAGTAGCATGGTTAGCAGGTC-3′	24
Beclin	Forward 5′-ACCGCAAGATTGTGGCTGAAGAC-3′	23
	Reverse 5′-TGAGCATAACGCATCTGGTTCTCC-3′	24
LC3-I	Forward 5′-GCTGCCAGTGCTGGACAAGAC-3′	21
	Reverse 5′-TCCTCATCCTTCTCCTGCTCGTAG-3′	24
LC3-II	Forward 5′-CCTGGTGCCAGATCACGTCAAC-3′	22
	Reverse 5′-AAGCCGTCCTCGTCCTTCTCG-3′	21
mTOR	Forward 5′-AACCACTGCTCGCCACAATGC-3′	21
	Reverse 5′-GATCGCCACACGGATTAGCTCTTC-3′	24
HK2	Forward 5′-TGGAGGTGAAGCGGAGGATGAG-3′	22
	Reverse 5′-GCACCAGCAGCACACGGAAG-3′	20
PK	Forward 5′-AAGTGACGCTGGACAATGCCTTC-3′	23
	Reverse 5′-CATGCCACCGTTCTCAACCTCAG-3′	23
SDH	Forward 5′-GTGGTGAAGGATCTCGTTCCAGAC-3′	24
	Reverse 5′-CAGGCACAGAGGATGCACTCATAG-3′	24
PDHX	Forward 5′-AGCTGTGCCTTCTGCTTATCCAAG-3′	24
	Reverse 5′-TGTCACAGTCAGCAGCAGCATATG-3′	24
AMPK	Forward 5′-TTGTATGCAGGCCCAGAGGT-3′	20
	Reverse 5′-TGGGATCCACCTGCAGCATA-3′	20
ATF6	Forward 5′-GGAAGGACTACGAGGTGATGATGC-3′	24
	Reverse 5′-GAGGACGAGCTGTAGAAGGTGTTG-3′	24
GRP78	Forward 5′-TCCTGCTCCTCGTGGTGTCC-3′	20
	Reverse 5′-CTCCTCTGGTGTTAGCCGATTCTG-3′	24
IRE1	Forward 5′-CAGAAGTGCCTCCTGCTGTTCC-3′	22
	Reverse 5′-GCTGTTGCTGATGTACGCTCATTG-3′	24
PERK	Forward 5′-GCCGTGGAGGTTTTGGAGTCG-3′	21
	Reverse 5′-CGCCTTGACTTCCCGCATCAC-3′	21
CHOP	Forward 5′-CAGCAGGAAGAAGAGCTGGC-3′	20
	Reverse 5′-CTGTCTGGGTCCAGGAGCTG-3′	20

particular protein has with others.

Statistical Analysis

We used IBM SPSS software (IBM SPSS Statistics 25.0) to analyze all data collected in our experiment. One-way ANOVA was employed to compare differences among groups. Two-way analysis of variance (ANOVA, test *F*) was employed to discern the possible interactions between NH_3 and LPS; *F* values having $P < 0.05$ were considered significant. Results were presented as mean ± standard deviation. Significant differences ($P < 0.05$) were indicated by different lowercase letters among groups.

Results

The effect of NH_3 and LPS on heart tissue structure

The ultrastructures of heart tissues from group C appeared normal. Numerous mitochondria (Mi) were arranged in an orderly manner, with clearly visible mitochondrial cristae (Cr). The myofilaments (My) were densely packed, and the sarcomeres (Sa) were distinctly discernible. The nuclei (N) appeared normal, featuring an intact bilayer nuclear membrane (NM), oval nucleoli (No), and evenly distributed chromatin (Ch) within the nucleus (Fig. 1a1-a2). In contrast, the other three groups displayed autophagic features under electron microscopy (Fig. 1 b1-b3). In groups N and P, autophagic vacuolar organelles (VOS) and autophagosomes (APS) were present, and mitochondrial vacuolation was also observed (Fig. 1b1-b2). In group NP, a significant number of VOs and APs were evident in cardiomyocytes, accompanied by more severe mitochondrial vacuolation (Fig. 1 b3). Apoptotic characteristics are

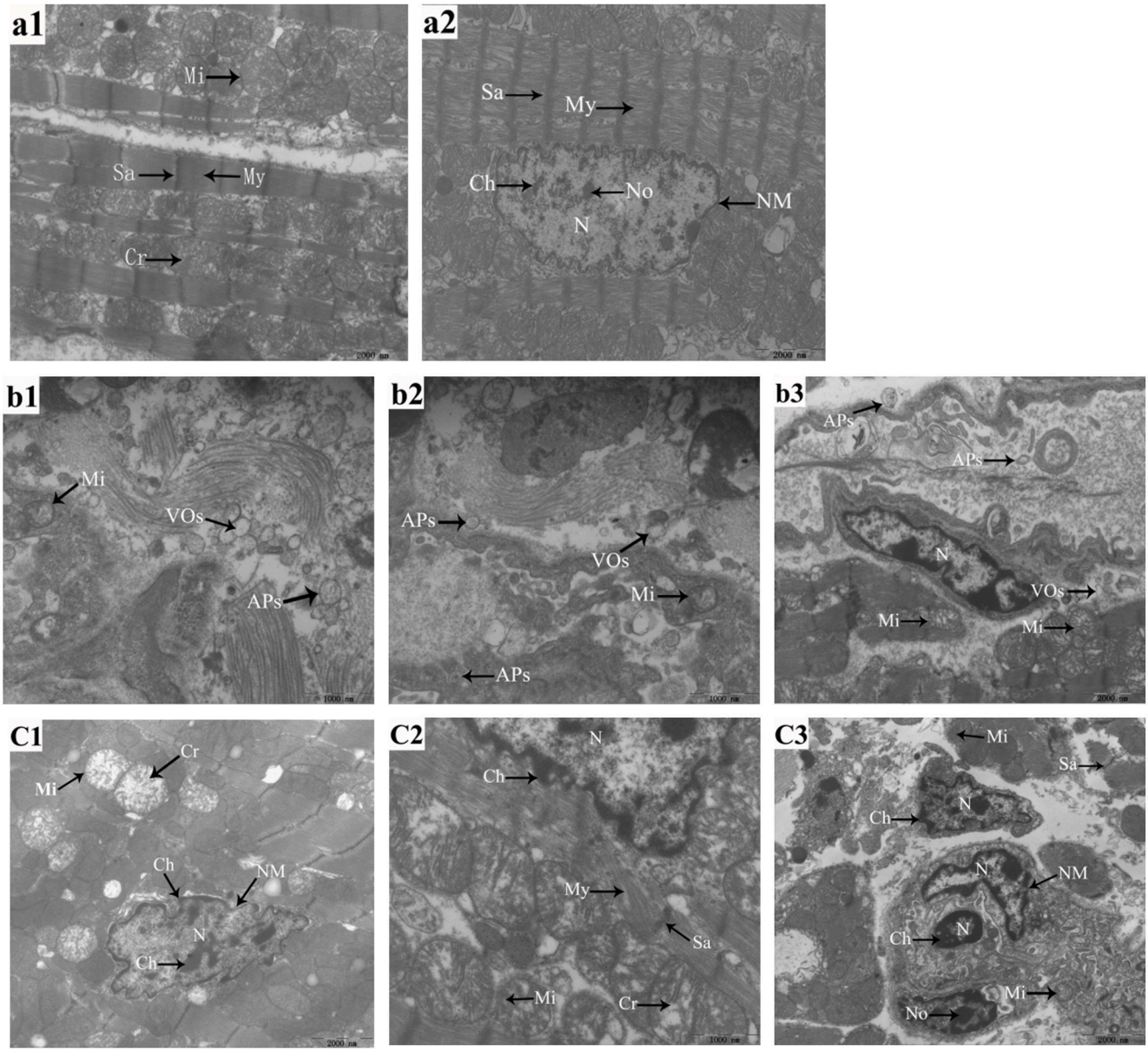

Fig. 1. Ultrastructure in the chicken cardiomyocyte. (a1) (a2) The group C (× 12000). (b1- b3) are autophagic ultrastructures. (c1-c3) is the ultrastructure of apoptosis. (b1) (c1) The group N (× 12000). (b2) (c2) group P (× 12000). (b3) (c3) The group NP (× 12000). Mi: mitochondria, Sa: sarcomeres, Cr: mitochondrial cristae, My: myofilaments, N: nucleus, NM: nuclear membrane, No: nucleolus, Ch: chromatin, VOs: vacuolar organelles, Aps: autophagosomes.

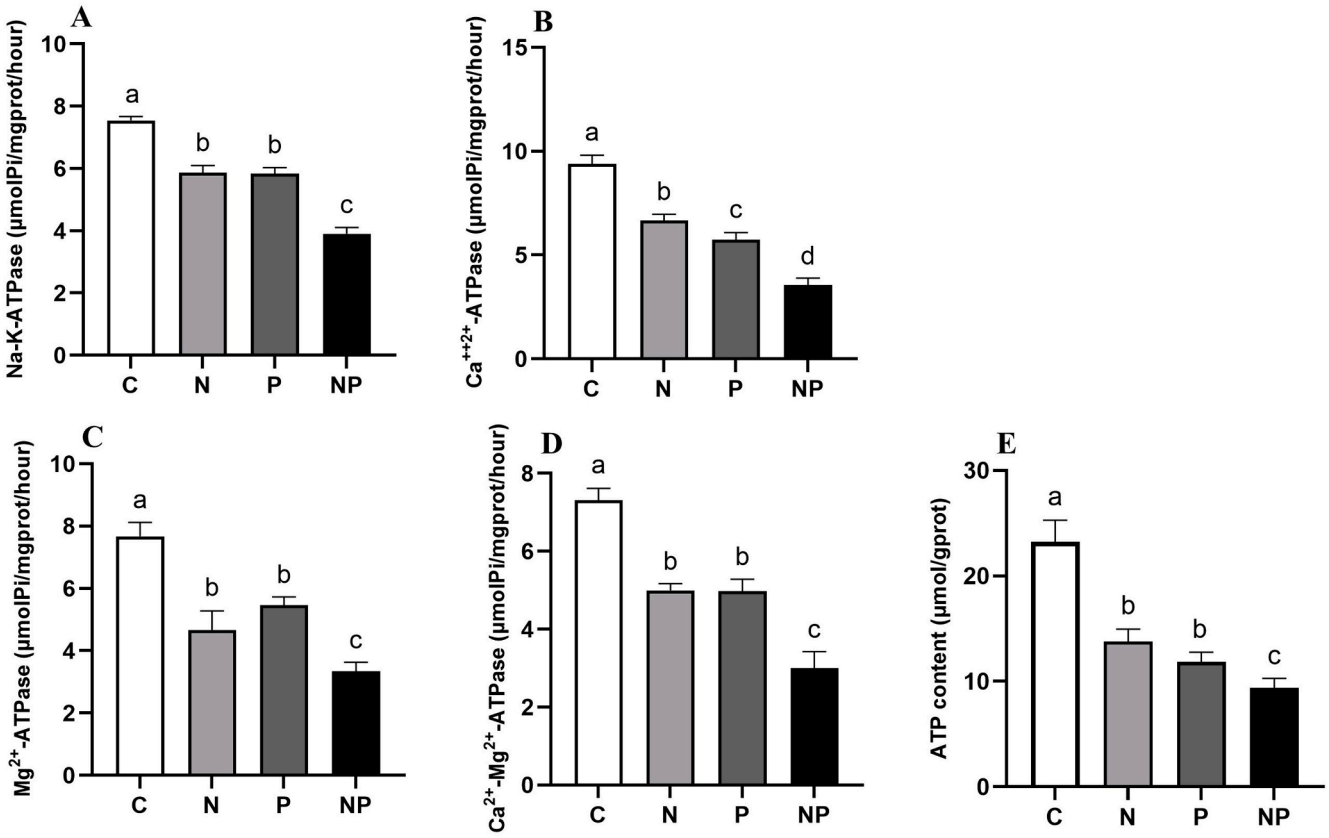

Fig. 2. (A-D) Activity of ATPase and (E) ATP content in heart tissue of chicken. Different lowercase letters indicate significant differences ($P < 0.05$) in different treated groups at the same gene expression. The data are shown as the mean ± SD.

illustrated in Fig. 1c1-c3. In groups N and P, some mitochondrial membranes were incomplete, the number of cristae decreased, myofibrils were disordered and sparse, and chromatin showed condensation, aggregation, and marginalization (Fig. 1c1-c2). In group NP, many mitochondrial membranes appeared indistinct, and cristae were fragmented or absent. Chromatin was aggregated in the nucleus along with significant chromatin marginalization, loosely arranged myofilaments, and prominent sarcomere rupture (Fig. 1b3).

The effects of NH_3 and LPS on ATPase activity and ATP content

In order to evaluate the effect of NH_3 or/and LPS on cardiac function, ATPase activity in the heart of chicken treated with NH_3 and LPS was measured and shown in Fig. 2A-D. Compared with group C, the activity of Na-K-ATPase, Ca^{++2+}-ATPase, Mg^{2+}-ATPase, and Ca^{2+}-Mg^{2+}-ATPase in the groups N, P, and NP significantly decreased, of which these ATPase activity in the group NP showed the most significant decrease. ATP content also showed the same trend. The ATP content in groups N, P, and NP was significantly lower than that in group C (Fig. 2E). There were no significant differences in the activity of Na-K-ATPase, Mg^{2+}-ATPase, and Ca^{2+}-Mg^{2+}-ATPase, or in ATP content, between the groups N and P. Moreover, as shown in Table 1S, the changes in ATPase activity at the co-exposure to NH_3 and LPS was due to an independent action of NH_3 and LPS, while ATP content at the co-exposure to NH_3 and LPS were due to an independent action of NH_3 and LPS as well as a result of an interaction between the two pollutants.

The effects of NH_3 and LPS on miR-1599 and HK2

We utilized the TargetScan database (http://targetscan.org/mamm_31/) to predict the target gene for miR-1599. The predicted binding site within the 3′ UTR region of HK2 for miR-1599 was depicted in Fig. 2A. The results indicated that HK2 serves as a target gene for miR-1599 in chickens.

The expression levels of miR-1599 and HK2 were shown in Fig. 2B and C, respectively. Compared to the control group, the expression level of miR-1599 in the treated group was significantly elevated ($P < 0.05$); however, no significant difference was observed between the groups N and P. Notably, the mRNA expression level in the group NP was significantly greater than that in the other groups ($P < 0.05$) (Fig. 2B). As shown in Fig. 2C, the mRNA expression of HK2 in the treated group was significantly downregulated compared to group C ($P < 0.05$). Among all groups, the group NP exhibited the lowest mRNA expression level of HK2, which was significantly lower than that of the other groups ($P < 0.05$). In addition, two-way ANOVA revealed that the changes in expression of miR-1599 and HK2 at the co-exposure to NH_3 and LPS were due to an independent action of NH_3 and LPS as well as a result of an interaction between the two pollutants (Table 2S).

The effects of NH_3 and LPS on energy metabolism

As shown in Fig. 3C-F, we found that mRNA expression levels of HK2, PK, PDHX, and SDH in groups N, P, and NP were significantly lower than those in group C. Compared to group C, the mRNA expression level of SDH in group NP showed the most significant decrease (Fig. 3F), whereas the mRNA expression level of HK2 exhibited the smallest decrease (Fig. 3C). Additionally, there were no significant differences in the mRNA expression levels of HK2 and PK between groups N and P (Fig. 3C–D), while the mRNA expression level of PDHK remained consistent across groups N, P, and NP (Fig. 3E). Additionally, compared to the control group, the mRNA expression level of AMPK was significantly increased ($P < 0.05$) in the NH_3-treated, LPS-treated, and NH_3+LPS-treated groups, the expression level of AMPK in group NP was significantly higher than those in the other groups (Fig. 3G). Moreover,

A

	Predicted consequential pairing of target region (top) and miRNA (bottom)
Position 24-30 of HK2 3' UTR	5' ...GGACUUCCUUCCCCGCUCCCUCC... 3'
gga-miR-1599	3' AAAAAAAAAAAGGAGGGAGG 5'

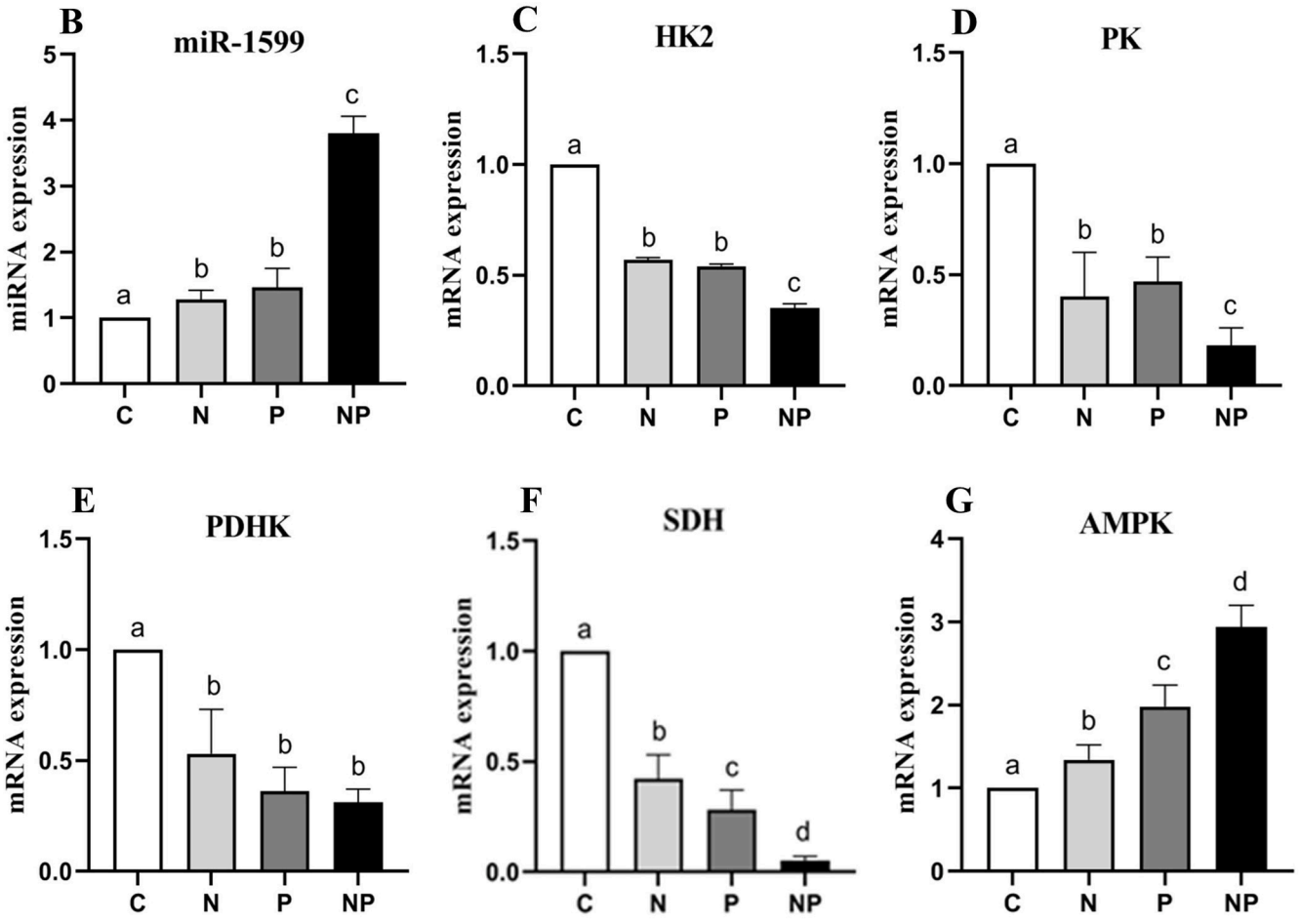

Fig. 3. (A) The Predicted binding sites of miR-1599 and its target gene HK2 in chicken. (B) Expression of miR-1599. (C-G) mRNA expression of energy metabolism-related genes in heart tissue of chicken. Different lowercase letters indicate significant differences ($P < 0.05$) in different treated groups at the same gene expression. The data are shown as the mean ± SD.

two-way ANOVA revealed that the expression changes in the energy metabolism-related genes in chicken cardiomyocytes co-exposed to NH_3 and LPS resulted from an independent action of NH_3 and LPS, as well as from interactions between the two toxic substances (Table 2S).

The effects of NH_3 and LPS on autophagy factors

To investigate the effects of NH_3 and LPS on autophagy in chicken heart tissues, we measured the mRNA levels of Beclin, mTOR, LC3-I, and LC3-II. As shown in Fig. 4A-D, the mRNA expression levels of Beclin, LC3-I, and LC3-II were significantly increased ($P < 0.05$) in groups N, P, and NP compared to group C. Notably, the mRNA expression levels of Beclin and LC3-I were significantly higher in group P compared to group N, and group NP exhibited the highest levels compared to both groups N and P (Fig. 4A–B). For LC3-II, the highest expression was observed in group NP, while no significant differences were found between groups N and P (Fig. 4C). Importantly, mTOR activity was suppressed in the experimental groups ($P < 0.05$), with group NP exhibiting significantly lower activity compared to the other groups (Fig. 4D). In addition, two-way ANOVA revealed that the changes of LC3-I and mTOR mRNA expression in chicken cardiomyocytes co-exposed to NH_3 and LPS resulted from an independent action of NH_3 and LPS as well as from interactions between the two toxic substances. In contrast, Beclin and LC3-II mRNA expression in group NP was influenced by the independent action of NH_3 and LPS (Table 3S).

The effects of NH_3 and LPS on ER stress

In Fig. 4E-4I, the real-time PCR results demonstrated elevated mRNA levels of ATF6, GRP78, IRE1, PERK, and CHOP, which are markers of ER stress. Compared to group C, the expression of these ER stress markers significantly increased in groups N, P, and NP ($P < 0.05$). For ATF6, GRP78, IRE1, and CHOP, no significant differences were found between the groups N and P; however, the group NP displayed significantly

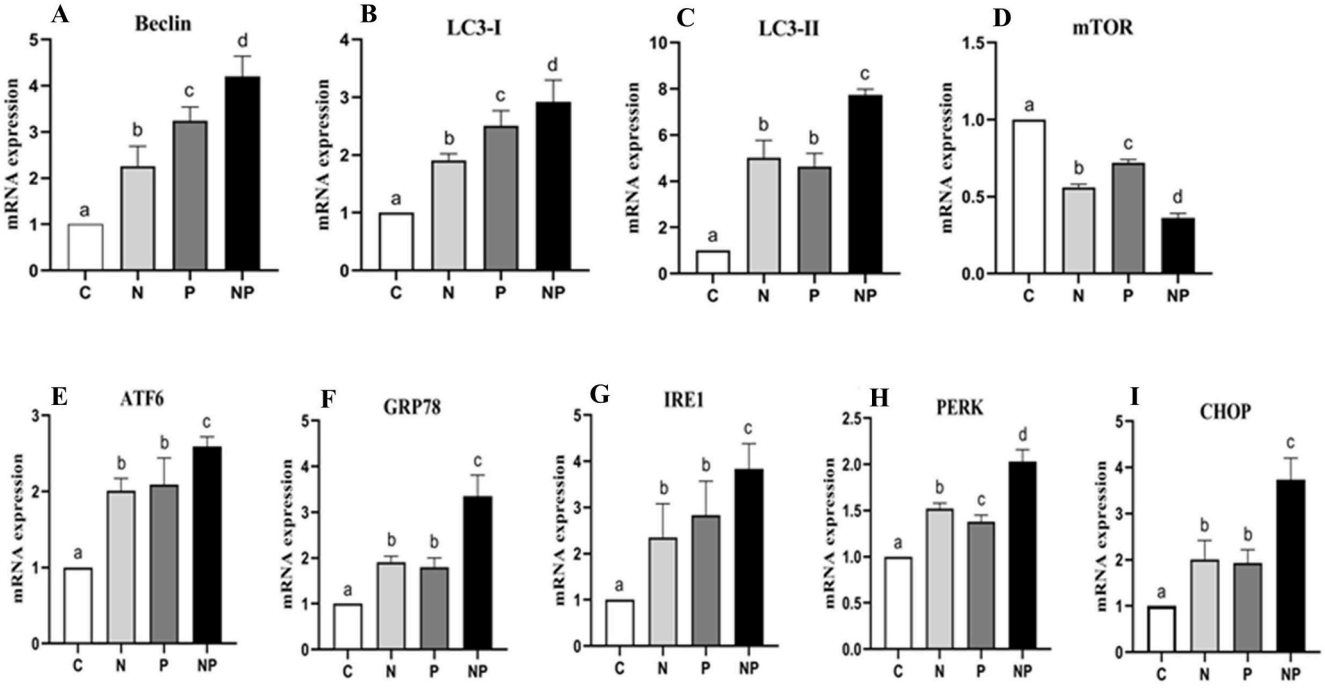

Fig. 4. (A-D) mRNA expression of autophagy-related genes in heart tissue of chicken. (E-I) mRNA expression of ER stress-related genes in heart tissue of chicken. Different lowercase letters indicate significant differences ($P < 0.05$) in the different treated groups at the same gene expression. The data are shown as the mean ± SD.

higher mRNA expression levels (Fig. 4E-G, I). As illustrated in Fig. 4H, the mRNA expression level of PERK in group NP was significantly greater than those in the other groups, with a notable difference also observed between the groups N and P ($P < 0.05$). In addition, two-way ANOVA revealed that the changes of ATF6, GRP78, IRE1, and PERK mRNA expression in chicken cardiomyocytes co-exposed to NH_3 and LPS resulted from an independent action of NH_3 and LPS, while CHOP mRNA expression resulted from an independent action of NH_3 and LPS as well as from interaction between two toxic substances (Table 4S).

The effects of NH_3 and LPS on apoptosis factors

Bim, Bax, Caspase-9, Caspase-3, and Bcl-2 were analyzed to investigate the effects of NH3 and LPS on apoptosis in chicken heart tissues. Compared to the control group, the expression levels of Bim, Bax, and Caspase-9 significantly increased in groups N, P, and NP ($P < 0.05$) (Fig. 5A–C). Caspase-3 mRNA expression also increased significantly in the experimental groups ($P < 0.05$); however, no significant differences were observed between groups P and NP (Fig. 5D). In contrast, Bcl-2 mRNA expression significantly decreased ($P < 0.05$) in the experimental groups compared to group C (Fig. 5E). It is interesting that apoptosis-related genes (Bim, Bax, Caspase-9, Caspase-3, and Bcl-2)

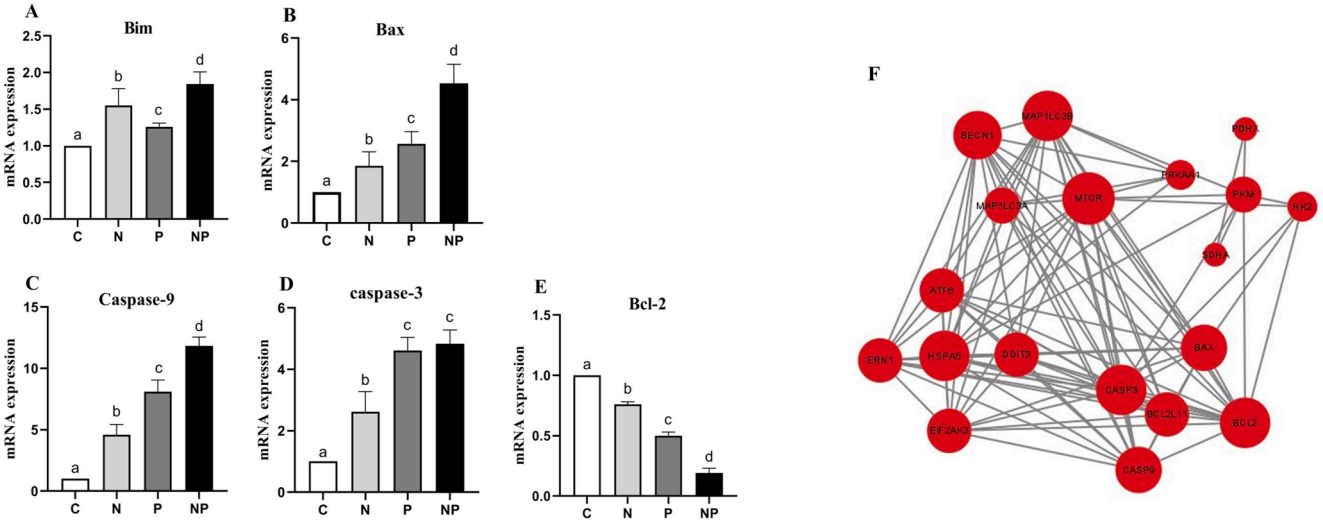

Fig. 5. (A-E) mRNA expression of apoptosis-related genes in heart tissue of chicken. Different lowercase letters indicate significant differences ($P < 0.05$) in the different treated groups at the same gene expression. The data are shown as the mean ± SD. (F) PPI network of energy metabolism, autophagy, ER stress, and apoptosis-related genes. Each node represents a gene name. The size of the nodes reflects the PPI degree of each term. The larger the node size, the larger the degree value.

expression in the NP group were influenced by the independent action of NH_3 and LPS (Table 5S).

The results of PPI analysis for energy metabolism, autophagy, ER stress, and apoptosis-related genes

As illustrated in Fig. 5F, the PPI network of genes associated with energy metabolism, autophagy, ER stress, and apoptosis demonstrated extensive interconnections, highlighting functional crosstalk among these mechanisms. Notably, mTOR exhibited the highest degree of connectivity within this network, emphasizing its central role and functional importance across these biological processes. This prominent connectivity underscores mTOR's potential regulatory influence on the interplay between these interconnected pathways.

Discussion

The heart is essential for sustaining the overall health and energy metabolism of chickens, making it crucial to investigate its response to environmental stressors. NH_3 and LPS are prevalent environmental pollutants in poultry farming, and previous studies indicated their adverse effects on cardiac function in chickens (Liu et al., 2020; Xing et al., 2019). Moreover, concurrent exposure to two pollutants may intensify their detrimental effects, ultimately compromising the overall health of chickens. In our experiment, NH_3 and LPS induced ER stress in chicken heart cells via impaired energy metabolism. Finally, it causes apoptosis and autophagy apoptosis and autophagy of cardiomyocytes. This effect is more pronounced when NH_3 and LPS work together.

Energy metabolism is essential for maintaining cardiac function in chickens, as it enables the heart to pump blood and meet the body's energy demands effectively. Cellular energy metabolism primarily occurs within the mitochondria and is influenced by the activity of ATPase, such as Na-K-ATPase, Ca^{++2+}-ATPase, Mg^{2+}-ATPase, and $Ca^{2+}Mg^{2+}$-ATPase. Our results demonstrated that both NH_3 or LPS induced mitochondrial damage and decreased activity of ATPase and ATP content in chicken cardiomyocytes, with their combined exposure exacerbating this injury and decrease, which indicated NH_3 or/and LPS decreased ATP generation, inducing impairment of energy metabolism in chicken hearts. HK2 and PK catalyze the production of intermediates that are essential substrates for ATP generation, playing an important role in subsequent ATP production within the TCA cycle (Chen et al., 2023b). PDHX catalyzes the conversion of pyruvate to acetyl-CoA, serving as a crucial substrate for the TCA cycle (Jiang et al., 2024), while SDH facilitates the conversion of succinate to fumarate within the cycle, further supporting ATP production (Moosavi et al., 2019). AMPK, as an energy-sensing kinase, is activated when ATP levels decrease (Garcia and Shaw, 2017). Thus, to further confirm our conclusion, we evaluated the mRNA expression levels of HK2, PK, PDHX, SDH, and AMPK, and our results indicated that both NH_3 and LPS decreased ATP generation, impaired energy metabolism in chicken hearts, with combined exposure to NH_3 and LPS leading to more severe effects. This finding further supported our conclusion that NH_3 or/and LPS led to a reduction in ATP production and impaired energy metabolism. Our findings align with those of previous studies. Chen et al. (2023a) reported that NH_3 exposure induced mitochondrial damage and reduced the activity of Na^+-K^+-ATPase, Ca^{2+}-ATPase, Mg^{2+}-ATPase, and $Ca^{2+}Mg^{2+}$-ATPase. Additionally, NH_3 exposure decreased the mRNA expression of HK2, PK, and SDH, ultimately leading to energy metabolism disturbances in chicken spleen lymphocytes. Excessive exposure to NH_3 caused a decrease in the levels of ATPase and ATP in pig hearts (Cheng et al., 2022). Similarly, Zhang et al. (2022c) found that NH_3 decreased HK2 mRNA expression while increasing AMPK mRNA expression, resulting in disrupted energy metabolism in pig hearts. In addition, Chi et al. (2018) found that hydrogen sulfide decreased the mRNA expression of HK2, PK, PDHX, and SDH, contributing to impaired energy metabolism in chicken peripheral blood lymphocytes.

A study showed that gga-miR-1599 is related to the development of chicken embryos (Huang et al., 2010), but the underlying mechanism remains unclear. In another experiment investigating the toxic effects of NH_3 on broilers, we analyzed the transcriptome data from chicken thymus, revealing that miR-1599 was significantly differentially expressed. Thus, we hypothesized that exposure to NH_3 and LPS induced alterations in gga-miR-1599 levels in chicken hearts and that gga-miR-1599 was implicated in the regulation of energy metabolism within this tissue. We used the TargetScan database to predict the target gene of miR-1599, and the results indicated that HK2 is one of its target genes. Our findings indicated that the expression level of miR-1599 in the experimental group was significantly higher than that in the control group. In contrast, the mRNA expression level of HK2 was significantly downregulated in the experimental group. Therefore, we speculated that NH_3 and LPS induced energy metabolism disorders in chicken cardiac myocytes via the gga-miR-1599/HK2 axis.

When cellular energy metabolism is disrupted, particularly in cases of insufficient ATP production, cells initiate autophagy to cope with energy deficiency (Yang et al., 2019). Our ultrastructural results demonstrated varying degrees of autophagic activity in chicken cardiomyocytes across all three experimental groups, with the most pronounced effects observed in the group exposed to both NH_3 and LPS (group NP). This indicated that the energy metabolism disorders induced by NH_3 and LPS may lead to the activation of autophagy. To validate this hypothesis, we further assessed the mRNA expression levels of autophagy-related genes, including mTOR, Beclin, LC3-I, and LC3-II. mTOR serves as a negative regulator of autophagy, inhibiting the process (Yang et al., 2019), while Beclin acts as an initiator of autophagy, contributing to the formation of autophagosomes (Prerna and Dubey, 2022). LC3 proteins are recognized as essential markers of autophagosome formation (Kuma et al., 2007). In our experiments, exposure to NH_3 and LPS resulted in the downregulation of mTOR and the upregulation of Beclin, LC3-I, and LC3-II mRNA expression levels. These findings suggested that exposure to NH_3 and LPS induced autophagy in chicken cardiomyocytes, with the combined exposure further exacerbating the autophagic process. Our findings were supported by research conducted by Chen et al. (2018), who demonstrated that cadmium exposure downregulated mTOR while upregulating LC3-I, LC3-II, and Beclin, thereby triggering autophagy in the spleens of chickens.

ER stress refers to the cellular stress response induced by the accumulation of unfolded or misfolded proteins in the ER. ATF6, IRE1, and PERK are the three primary sensors of ER stress, and their elevated expression indicates the presence of this stress (Sundaram et al., 2018; Liang et al., 2024). GRP78 promotes protein folding, and its expression is upregulated during ER stress (Liu et al., 2023). CHOP, a downstream effector of the PERK pathway, significantly increases in expression during severe ER stress (Hu et al., 2019). Previous studies showed that environmental pollutants, such as microplastics (Zhang et al., 2022d) and copper (Ma et al., 2023), can induce ER stress in chicken myocardium. However, it remains unclear whether ammonia NH_3 and LPS can induce ER stress in chicken hearts. Therefore, in our study, we assessed the mRNA expression levels of ER stress-related genes, including ATF6, IRE1, PERK, GRP78, and CHOP. Our results demonstrated that both NH_3 and LPS increased the mRNA expression of these genes, indicating that they induce ER stress in chicken cardiomyocytes, with combined exposure exacerbating the severity of this stress. These findings were consistent with previous studies. Hexavalent chromium exposure was shown to upregulate the expression of ATF6, IRE1, PERK, GRP78, and CHOP, thereby inducing ER stress in rat livers (Li et al., 2024). Similarly, cadmium exposure increased the expression of these genes, thereby triggering ER stress in chicken testicular stromal cells (Hou et al., 2023).

It is well-established that environmental stressors, including cytotoxic factors, pollutants, and toxins, can induce apoptosis and contribute to various pathological conditions (Franco et al., 2009). In our study, ultrastructural analysis revealed apoptotic features in cardiomyocytes exposed to NH_3 and LPS, with more pronounced effects observed under

combined exposure. This suggested that exposure to NH_3 and LPS may lead to apoptosis. To validate our findings, we further evaluated the mRNA expression levels of apoptosis-related genes, including Bim, Bax, Caspase-3, and Caspase-9. Bim and Bax are two pro-apoptotic factors, with Bim serving as an upstream activator of Bax (Chota et al., 2021). Caspase-9 is a key enzyme in the intrinsic apoptotic pathway, activating the downstream effector Caspase-3, thereby triggering the final steps of apoptosis (Brentnall et al., 2013). Conversely, Bcl-2, an anti-apoptotic protein, inhibits the activity of Bim and Bax, thereby preventing apoptosis (Qian et al., 2022). Our results indicated that both NH_3 and LPS induce apoptosis in chicken cardiomyocytes, as evidenced by the upregulation of Bim, Bax, Caspase-3, and Caspase-9 mRNA expression levels, along with a downregulation of Bcl-2 mRNA. Supporting our findings, previous studies indicated that polystyrene microplastics increased the expression of Caspase-9 and Caspase-3, thereby resulting in apoptosis in mouse testicular cells (Wen et al., 2023). Additionally, microplastics and di(2-ethylhexyl) phthalate elevated the expression of Bax, Caspase-3, and Caspase-9 while reducing Bcl-2 expression, thereby resulting in apoptosis in mouse pancreatic cells (Wang et al., 2022). Flurochloridone increased the expression of Bim and Bax, thereby inducing apoptosis in TM4 cells, a mouse testicular Sertoli cell line, via ER stress (Zhang et al., 2022a).

Cells experiencing environmental stress may simultaneously activate multiple response pathways, which frequently interact. For example, disrupted energy metabolism may trigger autophagy (Rong et al., 2022), which in turn can modulate ER stress levels and potentially lead to apoptosis (Kapuy, 2024). Our PPI analysis further revealed interactions among genes implicated in energy metabolism, autophagy, ER stress, and apoptosis. However, the precise mechanisms underlying energy metabolism disorders, autophagy, ER stress, and apoptosis induced by NH_3 and LPS in chicken cardiomyocytes remain unclear. Studies indicated that environmental pollutants can induce autophagy through the AMPK/mTOR signaling pathway. For instance, copper exposure induced autophagy in the livers of broiler chickens via the AMPK/mTOR pathway (Chen et al., 2024), while cadmium exposure induced autophagy in chicken spleens through the same pathway (Chen et al., 2018). In our study, we found that NH_3 and LPS induced energy metabolism disorders through the miR-1599/HK2 axis, which may subsequently lead to autophagy via the AMPK/mTOR pathway. Further research indicated that mTOR may play a regulatory role in ER stress; mTOR inhibitors upregulate PERK expression, thereby inducing ER stress in mouse intestinal endocrine cells (Freis et al., 2017). In T lymphocytes from mTOR-knockout mice, decreased mTOR expression correlates with increased IRE1 expression, which promotes ER stress (Bai et al., 2022). Therefore, our study suggested that the ER stress induced by NH_3 and LPS in chicken cardiomyocytes may be triggered by decreased mTOR expression. Additionally, studies showed that the ER stress-related gene CHOP is also a pro-apoptotic factor; it can downregulate Bcl-2 expression and upregulate Bim expression, resulting in increased Bax levels and ultimately triggering apoptosis (Hu et al., 2019). Wen et al. (2023) found that polystyrene microplastics increased the expression of CHOP, thereby inducing apoptosis in mouse testicular cells via ER stress. Wang et al. (2022) reported that elevated CHOP expression induced apoptosis in mouse pancreatic cells through ER stress. Zhang et al. (2022a) found that Flurochloridone increased CHOP expression, leading to apoptosis in TM4 cells, a mouse testicular Sertoli cell line, through ER stress.

Conclusion

In this study, we successfully established a toxicity model in chickens induced by NH_3 or/and LPS. As common environmental pollutants in poultry farming, our results indicate that both NH_3 and LPS induced impaired energy metabolism, autophagy, ER stress, and apoptosis in chicken hearts. Notably, combined exposure to these pollutants exacerbated the aforementioned processes. To our knowledge, this is the first report to examine the effects of combined NH_3 and LPS exposure on poultry. Through PPI analysis and assessments of the expression levels of relevant genes, we found that NH_3 or/and LPS induced impaired energy metabolism in chicken hearts via the miR-1599/HK2 axis, subsequently leading to autophagy through the AMPK/mTOR pathway. Furthermore, the decrease in mTOR expression induced by NH_3 or/and LPS triggered ER stress in chicken cardiomyocytes, ultimately leading to apoptosis through the increase of CHOP expression. This study provides new insights into the mechanisms by which combined exposure to NH_3 or/and LPS affects chickens, offering novel perspectives for mitigating the adverse effects of environmental pollutants on poultry.

Credit authorship contribution statement

Zhiyu Hao: Conceptualization, Data curation, Formal analysis, Investigation, Writing-original draft. **Minna Qiu:** Data curation, Formal analysis, Investigation. **Yuhao Liu:** Data curation, Investigation. **Yuhang Liu:** Data curation, Visualization. **Minghang Chang:** Data curation, Investigation. **Xiumei Liu:** Investigation, Software. **Yan Wang:** Investigation, Software. **Wei Sun:** Conceptualization, Investigation. **Xiaohua Teng:** Funding acquisition, Conceptualization, Supervision. **You Tang:** Methodology, Resources.

Declaration of competing interest

The authors declare that they have no known competing financial interests or personal relationships that could have appeared to influence the work reported in this paper.

Data availability

The data that has been used is confidential.

Acknowledgements

This work was supported by National Natural Science Foundation of China (No. 31972612), Academic Backbone fund of Northeast Agricultural University (20XG29), Postdoctoral scientific research developmental Fund of Heilongjiang Province (LBH-Z22066), Science and Technology Development Plan Project of Jilin Province (20240302074GX), and PhD Research Start-up Fund of Beihua University (0321/160324032).

Supplementary materials

Supplementary material associated with this article can be found, in the online version, at doi:10.1016/j.psj.2025.104965.

References

Bai, G., Wang, H., Cui, N., 2022. mTOR pathway mediates endoplasmic reticulum stress-induced CD4+ T cell apoptosis in septic mice. Apoptosis 27, 740–750.
Brentnall, M., Rodriguez-Menocal, L., De Guevara, R.L., Cepero, E., Boise, L.H., 2013. Caspase-9, caspase-3 and caspase-7 have distinct roles during intrinsic apoptosis. BMC Cell Biol. 14, 32.
Chen, C.Y., Zhang, S.L., Liu, Z.Y., Tian, Y., Sun, Q., 2015. Cadmium toxicity induces ER stress and apoptosis via impairing energy homoeostasis in cardiomyocytes. Biosci. Rep. 35.
Che, X., Xinchi Shang, WeiXu, Meiqi, X., Haiju, W., Wang Li, Li, Z., Geng, L., 2025. Selenium-enriched Lactiplantibacillus plantarum alleviates alkalinity stress-induced selective hepatic insulin resistance in common carp. International Journal of Biological Macromolecules 305, 141204.
Chen, D., Hu, G., Zhang, S., Zhang, H., Teng, X., 2020. Ammonia-triggered apoptosis via immune function and metabolic process in the thymuses of chickens by proteomics analysis. Ecotoxicol. Environ. Saf. 198, 110619.
Chen, D., Shen, F., Liu, J., Tang, H., Zhang, K., Teng, X., Yang, F., 2023a. The protective effect of Luteolin on chicken spleen lymphocytes from ammonia poisoning through mitochondria and balancing energy metabolism disorders. Poult. Sci. 102, 103093.
Chen, J., Liao, J.Z., Yu, W.L., Cao, H.B., Hu, G.L., Tang, Z.X., Al-Mutairi, K.A., Yang, F., 2024. Copper toxicity in the liver of broiler chicken: insights from metabolomics and AMPK-mTOR mediated autophagy perspective. Poult. Sci. 103.

Chen, M.H., Li, X.J., Fan, R.F., Yang, J., Jin, X., Hamid, S., Xu, S.W., 2018. Cadmium induces BNIP3-dependent autophagy in chicken spleen by modulating miR-33-AMPK axis. Chemosphere 194, 396–402.
Chen, S., Zou, Y., Song, C., Cao, K., Cai, K., Wu, Y., Zhang, Z., Geng, D., Sun, W., Ouyang, N., Zhang, N., Li, Z., Sun, G., Zhang, Y., Sun, Y., Zhang, Y., 2023b. The role of glycolytic metabolic pathways in cardiovascular disease and potential therapeutic approaches. Basic Res. Cardiol. 118, 48.
Chen, X., Shi, C., He, M., Xiong, S., Xia, X., 2023c. Endoplasmic reticulum stress: molecular mechanism and therapeutic targets. Signal. Transduct. Target. Ther. 8, 352.
Cheng, Z., Shu, Y., Li, X., Li, Y., Zhou, S., Liu, H., 2022. Evaluation of potential cardiotoxicity of ammonia: l-selenomethionine inhibits ammonia-induced cardiac autophagy by activating the PI3K/AKT/mTOR signaling pathway. Ecotoxicol. Environ. Saf. 233, 113304.
Chi, Q., Chi, X., Hu, X., Wang, S., Zhang, H., Li, S., 2018. The effects of atmospheric hydrogen sulfide on peripheral blood lymphocytes of chickens: perspectives on inflammation, oxidative stress and energy metabolism. Environ. Res. 167, 1–6.
Chota, A., George, B.P., Abrahamse, H., 2021. Interactions of multidomain pro-apoptotic and anti-apoptotic proteins in cancer cell death. Oncotarget 12, 1615–1626.
Franco, R., Sánchez-Olea, R., Reyes-Reyes, E.M., Panayiotidis, M.I., 2009. Environmental toxicity, oxidative stress and apoptosis: ménage à trois. Mutation Res. Genet. Toxicol. Environ. Mutagen. 674, 3–22.
Freis, P., Bollard, J., Lebeau, J., Massoma, P., Fauvre, J., Vercherat, C., Walter, T., Manié, S., Roche, C., Scoazec, J.-Y., Ferraro-Peyret, C., 2017. mTOR inhibitors activate PERK signaling and favor viability of gastrointestinal neuroendocrine cell lines. Oncotarget 8.
Garcia, D., Shaw, R.J., 2017. AMPK: mechanisms of cellular energy sensing and restoration of metabolic balance. Mol. Cell 66, 789–800.
Gargalionis, A.N., Papavassiliou, K.A., Papavassiliou, A.G., 2024. mTOR signaling: recent progress. Int. J. Mol. Sci. 25, 2587.
Ghareeb, K., Awad, W.A., BÖHm, J., Zebeli, Q., 2016. Impact of luminal and systemic endotoxin exposure on gut function, immune response and performance of chickens. World's. Poult. Sci. J. 72, 367–380.
Ghemrawi, R., Battaglia-Hsu, S.-F., Arnold, C., 2018. Endoplasmic reticulum stress in metabolic disorders. Cells 7, 63.
Han, Q., Tong, J.Y., Sun, Q., Teng, X.J., Zhang, H.F., Teng, X.H., 2020. The involvement of miR-6615-5p/Smad7 axis and immune imbalance in ammonia-caused inflammatory injury via NF-κb pathway in broiler kidneys. Poult. Sci. 99, 5378–5388.
He, M., Lu, Y., Xu, S., Mao, L., Zhang, L., Duan, W., Liu, C., Pi, H., Zhang, Y., Zhong, M., Yu, Z., Zhou, Z., 2014. MiRNA-210 modulates a nickel-induced cellular energy metabolism shift by repressing the iron–sulfur cluster assembly proteins ISCU1/2 in Neuro-2a cells. Cell Death. Dis. 5 e1090-e1090.
Hou, L.L., Wang, S.Z., Wang, Y.Y., Wang, M., Cui, Z.L., Huang, H., 2023. Antagonistic effect of selenium on programmed necrosis of testicular Leydig cells caused by cadmium through endoplasmic reticulum stress in chicken. Environ. Sci. Pollut. Res. 30, 112517–112535.
Hu, H., Tian, M., Ding, C., Yu, S., 2019. The C/EBP homologous protein (CHOP) transcription factor functions in endoplasmic reticulum stress-induced apoptosis and microbial infection. Front. Immunol. 9.
Huang, P., Gong, Y., Peng, X., Li, S., Yang, Y., Wang, X., Feng, Y., 2010. The expression profile analysis of sexual dimorphism miRNAs expressed in chicken embryo at the early stages of sex differentiation. J. Agric. Biotechnol. 18, 1149–1155.
Jiang, Z., Xiong, N., Yan, R., Li, S.-t., Liu, H., Mao, Q., Sun, Y., Shen, S., Ye, L., Gao, P., Zhang, P., Jia, W., Zhang, H., 2024. PDHX acetylation facilitates tumor progression by disrupting PDC assembly and activating lactylation mediated gene expression. Protein Cell.
Kapuy, O., 2024. Mechanism of decision making between autophagy and apoptosis induction upon endoplasmic reticulum stress. Int. J. Mol. Sci. 25, 4368.
Kolwicz, S.C., Purohit, S., Tian, R., 2013. Cardiac metabolism and its interactions with contraction, growth, and survival of cardiomyocytes. Circ. Res. 113, 603–616.
Kuma, A., Matsui, M., Mizushima, N., 2007. LC3, an autophagosome marker, can be incorporated into protein aggregates independent of autophagy: caution in the interpretation of LC3 localization. Autophagy 3, 323–328.
Li, X.Y., Li, N.N., Zhang, X.Z., Zhang, L.X., Jia, G., Yu, S.F., 2024. Low-dose hexavalent chromium exposure induces endoplasmic reticulum stress-mediated apoptosis in rat liver. Biol. Trace Elem. Res. 202, 4136–4145.
Liang, J., Lin, X., Jiang, C., Liu, Y., Hao, Z., Qiu, M., Liu, X., Chen, D., Teng, X., Tang, Y., 2024. Molecular mechanism of apoptosis induced by 4-tBP in common carp (Cyprinus carpio L.) head kidneys was explored from various angles: Hippo pathway, miR-203a, oxidative stress, ER stress, and mitochondrial pathway. Aquaculture 589, 740981.
Liao, J., Yang, F., Yu, W., Qiao, N., Zhang, H., Han, Q., Hu, L., Li, Y., Guo, J., Pan, J., Tang, Z., 2020. Copper induces energy metabolic dysfunction and AMPK-mTOR pathway-mediated autophagy in kidney of broiler chickens. Ecotoxicol. Environ. Saf. 206, 111366.
Liu, J., Wang, S.C., Zhang, Q.J., Li, X.J., Xu, S.W., 2020. Selenomethionine alleviates LPS-induced chicken myocardial inflammation by regulating the miR-128-3p-p38 MAPK axis and oxidative stress. Metallomics 12, 54–64.
Liu, Z., Liu, G., Ha, D.P., Wang, J., Xiong, M., Lee, A.S., 2023. ER chaperone GRP78/BiP translocates to the nucleus under stress and acts as a transcriptional regulator. In: Proceedings of the National Academy of Sciences, 120, e2303448120.
Ma, F.Y., Ma, X.Y., Yang, F., Liao, J.Z., Qiao, N., Yu, W.L., Han, Q.Y., Li, Y., Pan, J.Q., Hu, L.M., Guo, J.Y., Tang, Z.X., 2023. Exposure to copper induces endoplasmic reticulum (ER) stress-mediated apoptosis in chicken (*Gallus gallus*) myocardium. Vet. Res. Commun. 47, 2027–2040.
Ma, Y., Shi, Y.Z., Zou, X.T., Wu, Q.J., Wang, J.P., 2020. Apoptosis induced by mercuric chloride is associated with upregulation of PERK-ATF4-CHOP pathway in chicken embryonic kidney cells. Poult. Sci. 99, 5802–5813.
Moosavi, B., Berry, E.A., Zhu, X.-L., Yang, W.-C., Yang, G.-F., 2019. The assembly of succinate dehydrogenase: a key enzyme in bioenergetics. Cell. Mol. Life Sci. 76, 4023–4042.
Osorio Hernandez, R., Tinôco, I., Osorio Saraz, A., De, C., Coelho, R., Sousa, F., 2016. Calidad del aire en galpón avícola con ventilación natural durante la fase de pollitos. Agriambi 20, 660–665.
Pan, E.-Z., Xin, Y., Li, X.-Q., Wu, X.-Y., Tan, X.-L., Dong, J.-Q., 2023. Ameliorative effects of silybin against avermectin-triggered carp spleen mitochondrial dysfunction and apoptosis through inhibition of PERK-ATF4-CHOP signaling pathway. Fish. Physiol. Biochem. 49, 895–910.
Prerna, K., Dubey, V.K., 2022. Beclin1-mediated interplay between autophagy and apoptosis: new understanding. Int. J. Biol. Macromol. 204, 258–273.
Qian, S., Wei, Z., Yang, W., Huang, J., Yang, Y., Wang, J., 2022. The role of BCL-2 family proteins in regulating apoptosis and cancer therapy. Front. Oncol. 12.
Rong, Y., Zhang, S., Nandi, N., Wu, Z., Li, L., Liu, Y., Wei, Y., Zhao, Y., Yuan, W., Zhou, C., Xiao, G., Levine, B., Yan, N., Mou, S., Deng, L., Tang, Z., Liu, X., Kramer, H., Zhong, Q., 2022. STING controls energy stress-induced autophagy and energy metabolism via STX17. J. Cell Biol. 221.
Smit, L.A.M., Boender, G.J., de Steenhuijsen Piters, W.A.A., Hagenaars, T.J., Huijskens, E.G.W., Rossen, J.W.A., Koopmans, M., Nodelijk, G., Sanders, E.A.M., Yzermans, J., Bogaert, D., Heederik, D., 2017. Increased risk of pneumonia in residents living near poultry farms: does the upper respiratory tract microbiota play a role? Pneumonia 9, 3.
Sundaram, A., Appathurai, S., Plumb, R., Mariappan, M., 2018. Dynamic changes in complexes of IRE1α, PERK, and ATF6α during endoplasmic reticulum stress. Mol. Biol. Cell 29, 1376–1388.
Van Damme, M., Clarisse, L., Whitburn, S., Hadji-Lazaro, J., Hurtmans, D., Clerbaux, C., Coheur, P.-F., 2018. Industrial and agricultural ammonia point sources exposed. Nature 564, 99–103.
Vučemilo, M., Matković, K., Vlnković, B., Jakšić, S., Granić, K., Mas, N., 2007. The effect of animal age on air pollutant concentration in a broiler house. Czech J. Anim. Sci. 52, 170–174.
Wang, S., Xu, Z., Yin, H., Min, Y., Li, S., 2018a. Alleviation mechanisms of selenium on cadmium-spiked in chicken ovarian tissue: perspectives from autophagy and energy metabolism. Biol. Trace Elem. Res. 186, 521–528.
Wang, X.Y., An, Y., Jiao, W.Y., Zhang, Z.Y., Han, H., Gu, X.H., Teng, X.H., 2018b. Selenium protects against lead-induced apoptosis via endoplasmic reticulum stress in chicken kidneys. Biol. Trace Elem. Res. 182, 354–363.
Wang, Y., Zhang, Y., Sun, X., Shi, X., Xu, S., 2022. Microplastics and di (2-ethylhexyl) phthalate synergistically induce apoptosis in mouse pancreas through the GRP78/CHOP/Bcl-2 pathway activated by oxidative stress. Food Chem. Toxicol. 167, 113315.
Wen, S., Chen, Y., Tang, Y., Zhao, Y., Liu, S., You, T., Xu, H., 2023. Male reproductive toxicity of polystyrene microplastics: study on the endoplasmic reticulum stress signaling pathway. Food Chem. Toxicol. 172, 113577.
Wyer, K.E., Kelleghan, D.B., Blanes-Vidal, V., Schauberger, G., Curran, T.P., 2022. Ammonia emissions from agriculture and their contribution to fine particulate matter: A review of implications for human health. J. Environ. Manage 323, 116285.
Xing, H.J., Peng, M.Q., Li, Z., Chen, J.Q., Zhang, H.F., Teng, X.H., 2019. Ammonia inhalation-mediated mir-202-5p leads to cardiac autophagy through PTEN/AKT/mTOR pathway. Chemosphere 235, 858–866.
Yang, J., Zhou, R., Ma, Z., 2019. Autophagy and energy metabolism. In: Qin, Z.-H. (Ed.), Autophagy: Biology and Diseases: Basic Science. Springer Singapore, Singapore, pp. 329–357.
Yang, J.X., Rastetter, R.H., Wilhelm, D., 2016. Non-coding RNAs: an introduction. In: Wilhelm, D., Bernard, P. (Eds.), Non-coding RNA and the Reproductive System. Springer, Netherlands, Dordrecht, pp. 13–32.
Zhang, F., Ni, Z.J., Zhao, S.Q., Wang, Y.N., Chang, X.L., Zhou, Z.J., 2022a. Flurochloridone induced cell apoptosis via ER stress and eIF2α-ATF4/ATF6-CHOP-bim/bax signaling pathways in mouse TM4 sertoli cells. Int. J. Environ. Res. Public Health 19.
Zhang, J., Guo, J., Yang, N., Huang, Y., Hu, T., Rao, C., 2022b. Endoplasmic reticulum stress-mediated cell death in liver injury. Cell Death. Dis. 13, 1051.
Zhang, X., Wang, A., Wang, X., Zhao, Q., Xing, H., 2022c. Evaluation of L-selenomethionine on ameliorating cardiac injury induced by environmental ammonia. Biol. Trace Elem. Res. 200, 4712–4725.
Zhang, Y., Wang, D.X., Yin, K., Zhao, H.J., Lu, H.M., Meng, X., Hou, L.L., Li, J.B., Xing, M. W., 2022d. Endoplasmic reticulum stress-controlled autophagic pathway promotes polystyrene microplastics-induced myocardial dysplasia in birds. Environ. Pollut. 311.
Zheng, X., Guo, C., Lv, Z., Li, J., Jiang, H., Li, S., Yu, L., Zhang, Z., 2024. Novel findings from arsenic-lead combined exposure in mouse testicular TM4 Sertoli cells based on transcriptomics. Sci. Total. Environ. 913, 169611.
Zhou, Q., Hao, Z., Qiu, M., Liu, Y., Chang, M., Liu, X., Wang, Y., Tang, Y., Sun, W., Teng, X., Liu, Y., 2025. Amino acid metabolism disorder and oxidative stress took part in EGCG alleviating Mn-caused ferroptosis via miR-9–5p/got1 axis. Journal of Hazardous Materials 489, 137656.